A New Light Source of VLC Combining White LEDs and RGB LEDs

Jian Song[1], Wensheng Zhang[1], Li Zhou[1], Xiaotian Zhou[1], Jian Sun[1], and Cheng-Xiang Wang[2]
[1]Shandong Provincial Key Lab of Wireless Communication Technologies,
School of Information Science and Engineering, Shandong Univiersity, Jinan, Shandong, 250100, P.R.China.
[2]Institute of Sensors, Signals and Systems, School of Engineering & Physical Sciences,
Heriot-Watt University, Edinburgh, EH14 4AS, UK.
Email: songjianyear@163.com, zhangwsh@sdu.edu.cn, zhou_li@sdu.edu.cn,
xtzhou@sdu.edu.cn, sunjian@sdu.edu.cn, cheng-xiang.wang@hw.ac.uk

***Abstract*—In this paper, a new light source of visible light communication (VLC) systems is firstly proposed for illumination and data transmission simultaneously. The new light source is composed of white light emitting diodes (LEDs) and one or more sets of red, green, and blue (RGB) LEDs. White LEDs provide the function of illumination, while RGB LEDs are utilized as antennas for information transmission. There are seven combinations of RGB LEDs used for communication. Six of the seven combinations are investigated except the combination of RGB LEDs, which are introduced in detail in the scenario and light source model. Firstly, we investigate the quality of light source using the color rendering index (CRI) of light source. The signal-to-noise ratio (SNR) of the receiver is analyzed theoretically from the perspective of communication. Finally, we analyze the power ratio of RGB LEDs and white LEDs under the constraints of CRI, SNR, and bit error rate (BER). The simulation results show that the new light source can be used for VLC. The power of the RGB LEDs can be adjusted to meet the communication and illumination needs of different scenarios.**

***Index Terms*—VLC, RGB LEDs,white LEDs,power ratio,SNR.**

I. Introduction

Over the past few years, wireless communications have been facing an increasingly serious spectrum crisis. VLC occupies an extremely rich spectrum resource from 400 THz to 800 THz [1]. VLC utilizes white LEDs or RGB LEDs to offer dual functions of data transmission and illumination simultaneously. What's more, it has become an attractive and promising technology to enhance the performance of conventional wireless communication systems [2]. VLC is playing an important role in the next generation of wireless communications, especially as an alternate of indoor high-speed wireless access.

Compared to the radio frequency (RF) wireless communication, VLC offers the advantageous properties of the high efficiency, immunity to electromagnetic interference, high security, frequency license free, and relatively high modulation bandwidth. Thus, it supports high quality communication at a high data rate and has very wide and biologically friendly applications [3]. In general, VLC as short-range optical wireless communication realizes communication function through modulating the light intensity of LEDs at the transmitter. At the receiver, the photo-detector (PD) converts the optical intensity into electrical current [2].

There have been many investigations on VLC systems. Different categories of LEDs used for VLC systems were introduced in [2] and recent representative research about VLC were summarized in [4]. However, most of the investigations focus on white LEDs or RGB LEDs used in VLC systems. The combination of the two kinds of light source are still missing in the literature.

The VLC system generally uses two traditional ways to obtain the white light for illumination function. One of the most commonly used methods is to combine one blue emitter with yellow phosphor to get the white light, the other is to combine the light from the three primary colors (red, green, and blue) to generate white light [5]. The former has a great advantage on the illumination. However, the bottleneck for white LEDs is that the low response speed of the phosphor-based emitters limits the communication bandwidth and data rate of VLC systems [6]. The latter spends too much cost from the point of view of illumination, but RGB LEDs are considered as a strong candidate for communication devices. Because RGB LEDs can apply wavelength division multiplexing (WDM) and multiple-input-multiple-output (MIMO) technology in VLC systems. These technology can provide multiple independent communication channels to improve the data rate and the capacity of the VLC systems [7].

To the best of our knowledge, it is the first VLC system which combines the white LEDs responsible for illumination and RGB LEDs used for communication. What's more, it can avoid the problem of illumination flickering. In order to better realize functions of illumination and communications, the relationship between them should be investigated. The influence of different combinations of RGB LEDs used as antennas on the illumination of white LEDs is theoretically analyzed. At the same time, the effect of lighting on communication is also studied. The available power ratio of RGB LEDs and white LEDs from the point of view of CRI, SNR, and BER of the VLC system are investigated.

The rest of this paper is organized as follows. Section II describes the scenario and light source model. The tristimulus values of light source and color rendering index are

978-1-5386-4502-4/17/$31.00 ©2017 IEEE

also introduced in this section. The optical channel model, SNR of receiver, and optimal power ratio are investigated in Section III. The numerical and simulation results are given in Section IV. Finally, Section V shows the conclusions.

II. System Model

A. The Scenario and Light Source Model

The room size is 4×4×3 m^3 as shown in Fig. 1. The light source is installed at the middle of the roof. A PD is placed on a 0.85 m high desk and connected to a computer. The vertical distance between the transmitter and receiver is h. The new light source model is also shown in Fig. 1. It is made of white LEDs and a set or more sets of RGB LEDs. The outer ring is the white LEDs, which is utilized to provide stable lighting. A stable lighting can keep human eyes free from the illumination flickering. The middle is the location of the RGB LEDs, which is used as antennas to transmit the optical signal through free optical channel. When analyzing the impact of communication on lighting, we need to get the spectral distribution of light source. There are many mathematical LED spectrum models describing the spectral power distribution (SPD) of a LED. To simulate multichip LEDs, double Gaussian model is used to describe the actual LED spectrum. The model of a LED is given by [8], [9]

$$S_{\text{LED}}(\lambda) = g(\lambda, \lambda_0, \Delta\lambda_{0.5}) + \frac{2}{3}g^5(\lambda, \lambda_0, \Delta\lambda_{0.5}) \quad (1)$$

$$g(\lambda, \lambda_0, \Delta\lambda_{0.5}) = \exp(-(\frac{\lambda-\lambda_0}{\Delta\lambda_{0.5}})^2) \quad (2)$$

where $S_{\text{LED}}(\lambda)$ is the SPD of a LED, the wavelength of light, the peak wavelength, and the full width half maximum (FWHM) are λ, λ_0, and $\Delta\lambda_{0.5}$, respectively. From this model, we can simulate the SPD of the new light source. After the normalization processing, the SPD of the new light soure can be given by

$$S_{\text{Light}}(\lambda) = S_{\text{White}}(\lambda) + \eta S_{\text{LED}}(\lambda) \quad (3)$$

$$\eta = \frac{P_{\text{LED}}}{P_{\text{White}}} \quad (4)$$

where $S_{\text{White}}(\lambda)$ is the SPD of white LEDs, which is measured in [10]. The power of red, green, or blue LEDs is P_{LED}. The power of white LEDs is P_{White}. The power of red, green, or blue LEDs to the power of white LEDs ratio is η. The $S_{\text{LED}}(\lambda)$ has seven kinds of combinations of red LEDs, green LEDs, blue LEDs, red + green LEDs, red + blue LEDs, green + blue LEDs, and red + green + blue LEDs.

B. Values of Light Source

When the three primary colors are determined, the tristimulus values of one color are unique. Therefore, the tristimulus values represent the color. In 1931, International Commission of Illumination (CIE) adopted a new color system named 1931 CIE XYZ system. The color of the light source can be determined by the CIE 1931 chromaticity coordinates (x, y), which is a u-shaped curve [11]. For determining the color of the light source, we firstly need to calculate the trisitimulus values of light source. According to (3), the three values of the new light source are given by

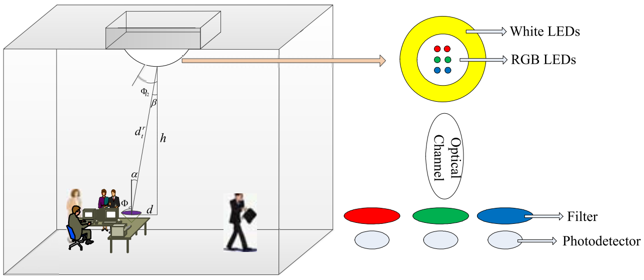

Fig. 1. The scenario and light source model.

$$X_{\text{light}} = k\int_{380}^{780} S_{\text{Light}}(\lambda)\overline{x}(\lambda)d\lambda \quad (5)$$

$$Y_{\text{light}} = k\int_{380}^{780} S_{\text{Light}}(\lambda)\overline{y}(\lambda)d\lambda \quad (6)$$

$$Z_{\text{light}} = k\int_{380}^{780} S_{\text{Light}}(\lambda)\overline{z}(\lambda)d\lambda \quad (7)$$

where $\overline{x}(\lambda)$, $\overline{y}(\lambda)$, and $\overline{z}(\lambda)$ are the color matching functions derived from average data of the CIE 1931 standard colorimetric observer. Here, k is a normalizing constant, when $S_{\text{Light}}(\lambda)$ is achieved in an absolute unit, $k = 683$ lm/W. According to these tristimulus values, the color point coordinate $(x_{\text{light}}, y_{\text{light}})$ of light source is given by [11], [12]

$$x_{\text{light}} = \frac{X_{\text{light}}}{X_{\text{light}} + Y_{\text{light}} + Z_{\text{light}}} \quad (8)$$

$$y_{\text{light}} = \frac{Y_{\text{light}}}{X_{\text{light}} + Y_{\text{light}} + Z_{\text{light}}} \quad (9)$$

$$z_{\text{light}} = 1 - x_{\text{light}} - y_{\text{light}}. \quad (10)$$

However, color is not evenly distributed in chromaticity coordinates (x, y). In 1960, the CIE developed the chromaticity diagram and gave a uniform chromaticity coordinates named CIE 1960 (u, v) [12]. The chromaticity coordinates $(u_{\text{light}}, v_{\text{light}})$ are given by

$$u_{\text{light}} = \frac{4x_{\text{light}}}{-2x_{\text{light}} + 12y_{\text{light}} + 3} \quad (11)$$

$$v_{\text{light}} = \frac{6y_{\text{light}}}{-2x_{\text{light}} + 12y_{\text{light}} + 3}. \quad (12)$$

In the distribution of colors, CIE 1960 (u, v) is more advantageous than chromaticity coordinates (x, y).

C. CRI

In order to measure the quality of the light source, the CIE defined the CRI which is the only internationally recognized standard of color rendering evaluation [9]. CRI has the special CRI (R_i) and the general CRI (R_a). The new light source is compared to a standard reference light source under the condition of the same correlated color temperature (CCT) [13] and 14 kinds of test samples of color named Munsell samples, $\mathrm{R_i}$ is given by

$$\mathrm{R_i} = 100 - 4.6\Delta E_i \quad (i = 1, \ldots, 14) \tag{13}$$

where ΔE_i is the color difference between light source and a standard reference light source in 1964 unified space coordinate system. The first eight kinds of test samples of color are used to evaluate the light source and defined as

$$\mathrm{R_a} = \sum_{i=1}^{8} (\mathrm{R_i}/8). \tag{14}$$

The larger value of $\mathrm{R_a}$ is, the closer to the standard light source. When $\mathrm{R_a}$=100, the light source is the same as the standard light source.

III. Communication Performance Analysis

A. Optical Channel Model

In optical link, information is transmitted to the receiver by the optical signal intensity from RGB LEDs. Although the optical wireless channel includes both line-of-sight (LOS) and multipath components, it has been reported that the power of LOS is much higher than the power from the reflected path. Therefore, only LOS propagation path is considered in this VLC system and the direct current (DC) gain is written as [14]

$$H_{\mathrm{LOS}}^{\mathrm{LED}} = \frac{(l+1)A_{\mathrm{PDA}}}{2\pi d_{\mathrm{t}}^{\mathrm{r}\,2}} \cos^l(\beta)\cos(\alpha)T(\alpha)G(\alpha)judg(\tfrac{\alpha}{\Phi_c}) \tag{15}$$

$$d_{\mathrm{t}}^{\mathrm{r}} = d^2 + h^2 \tag{16}$$

where A_{PDA} is the area of the PD at the receiver. The horizontal distance and the distance between transmitter and receiver, are d and $d_{\mathrm{t}}^{\mathrm{r}}$, respectively. The angle of incidence, the angle of irradiance, the semiangle at half power, and the field of view (FOV) at the receiver are α, β, $\Phi_{1/2}$, and Φ_c, respectively. The gain of an optical filter is $T(\alpha)$ and generally takes the value of 1. The angle-dependent radiation pattern is $(l+1)\cos^l(\beta)/2\pi$ and l is the Lambertian index and given by $l = -\ln 2/\ln(\cos\Phi_{1/2})$. $G(\alpha)$ is the gain of an optical concentrator and it is written as

$$G(\alpha) = \begin{cases} \frac{c^2}{\sin^2(\Phi_c)}, & 0 \le \alpha \le \Phi_c \\ 0, & \alpha > \Phi_c \end{cases} \tag{17}$$

where c is the refractive index. $judg()$ is a decision function and given by

$$judg(\frac{\alpha}{\Phi_c}) = \begin{cases} 1, & |\frac{\alpha}{\Phi_c}| \le 1 \\ 0, & |\frac{\alpha}{\Phi_c}| > 1. \end{cases} \tag{18}$$

B. SNR and Noise Analysis

In this VLC system, the technology of direct current optical orthogonal frequency division multiplexing (DCO-OFDM) is used in our analysis. The SNR of the optical channel is analyzed. The noise in VLC mainly consists of shot noise, thermal noise, and amplifier noise [16]–[18]. The received optical signal power from the RGB LEDs is independent of the red, green, and blue components of the white LED. Since the power of the red, green, and blue components of the white LEDs is a constant, it does not have any effect on the strength of optical signal from RGB LEDs after filtering the direct current components and just contributes to the shot noise. The received average optical signal power is given by

$$\overline{P}_{\mathrm{r}}^{\mathrm{X}} = \frac{1}{B} P_{\mathrm{T}}^{\mathrm{X}} H_{\mathrm{LOS}}^{\mathrm{LED}} \int_0^B G_{\mathrm{T}}(f)df \tag{19}$$

$$P_{\mathrm{T}}^{\mathrm{X}} = \eta P_{\mathrm{White}} \tag{20}$$

where $P_{\mathrm{T}}^{\mathrm{X}}$ is the optical power from red, green, or blue LED. X represents the red, green, or blue component from RGB LEDs. B is the bandwidth of system. $G_{\mathrm{T}}(f)$ is the power spectrum density of frequency response of a LED. The SNR can be used to measure the quality of communication and it is defined as

$$SNR^{\mathrm{X}} = \frac{(R\overline{P}_{\mathrm{r}}^{\mathrm{X}})^2}{\sigma_{total}^2} \tag{21}$$

$$\sigma_{total}^2 = P_{\mathrm{Rshot}}^2 + P_{\mathrm{Rthermal}}^2 + P_{\mathrm{Ramp}}^2 \tag{22}$$

where R is the responsivity of the PD. At the receiver, the received electrical signal is affected by shot noise, thermal noise, and amplifier noise. Shot noise variance is given by

$$P_{\mathrm{Rshot}}^2 = 2qR\overline{P}_{\mathrm{r}}B + 2qI_{\mathrm{BC}}I_2B \tag{23}$$

where q is the electronic charge. I_{BC} is the background current. I_2 is a noise bandwidth factor, generally takes the value of 0.562. $\overline{P}_{\mathrm{r}}$ is the received average optical power from RGB LEDs and white LEDs. It is defined as

$$\overline{P}_{\mathrm{r}} = \overline{P}_{\mathrm{r}}^{\mathrm{X}} + H_{\mathrm{LOS}}^{\mathrm{LED}} \frac{P_{\mathrm{White}} \int_{\mathrm{X}} S_{\mathrm{White}}^{\mathrm{X}}(\lambda)d\lambda}{\int_{380}^{780} S_{\mathrm{White}}(\lambda)d\lambda} \tag{24}$$

where $S_{\mathrm{White}}^{\mathrm{X}}$ represents the red, green, or blue components of white light from white LEDs. The thermal noise variance and the amplifier noise variance are given by [17] [18]

$$P_{\mathrm{Rthermal}}^2 = 8\pi\kappa_{\mathrm{B}}T\frac{\mu A_{\mathrm{PDA}}I_2B^2}{G_{\mathrm{o}}} + 16\pi^2\kappa_{\mathrm{B}}T\vartheta\frac{\mu^2 A_{\mathrm{PDA}}I_3B^3}{g_{\mathrm{m}}} \tag{25}$$

$$P_{\mathrm{Ramp}}^2 = i_{\mathrm{amp}}^2 B \tag{26}$$

where κ_{B} is Boltzman's constant. μ is the fixed capacitance of PD per unit area. T is absolute temperature. G_{o} is the open-loop voltage gain. ϑ is the field effect transistor (FET) channel noise factor. g_{m} is the FET transconductance. i_{amp} is the amplifier noise density. I_3 is the noise bandwidth factor for a full, raised-cosine, equalized pulse shape, generally takes the value of 0.0868 [19].

C. Optimal Power Ratio

For indoor lighting, when a modulation method is used in a VLC system, the minimum SNR and the maximum BER of system need to meet the communication requirements. The SNR^{X} and $BER_{\max}$ can be determined by the numerical results or simulation results. Simulation results are used in

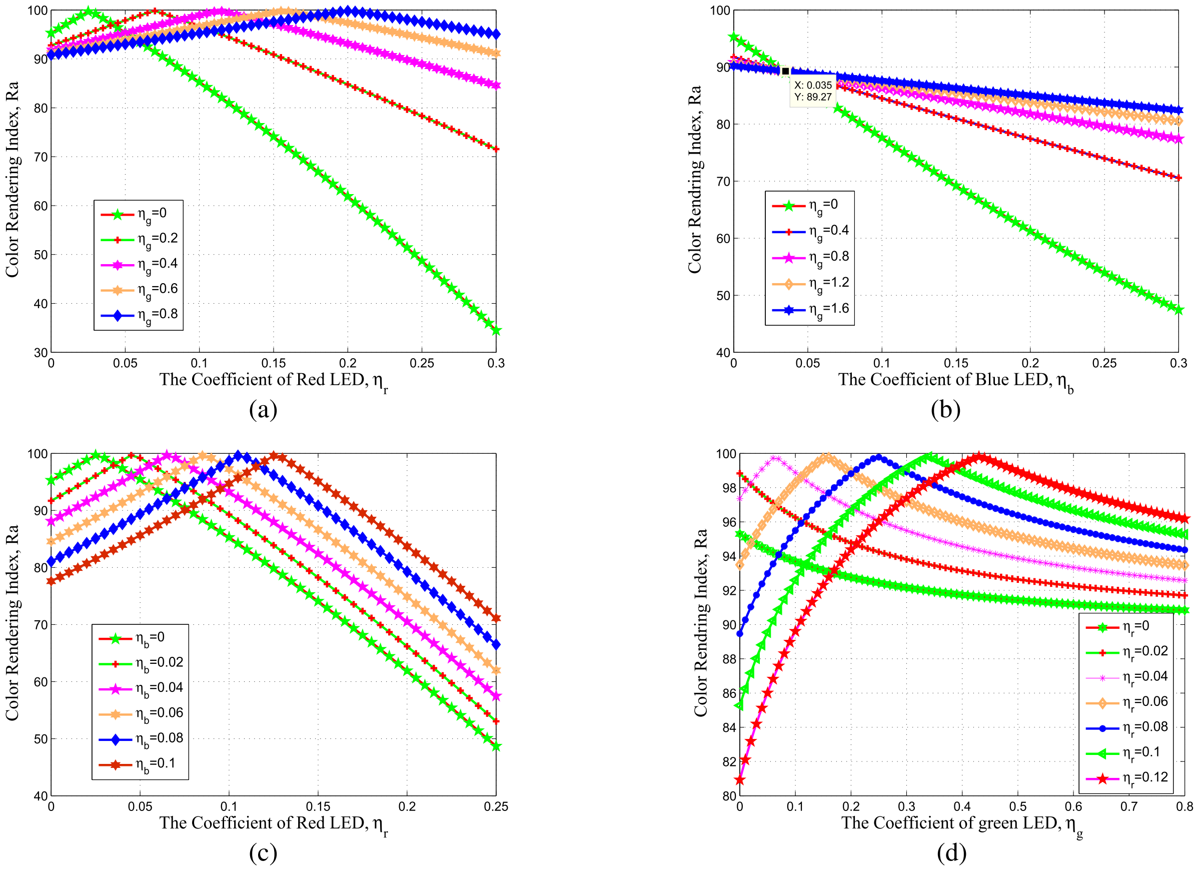

Fig. 2. The CRI of the new light source with different combinations. (a) combine red and green LEDs, (b)combine blue and green LEDs, (c) combine red and blue LEDs, and (d) combine green and red LEDs.

our analysis. When on-off keying (OOK) modulation is used in VLC systems, the minimum SNR of system is 15.6 dB when BER is 10^{-6}[18].

In order to ensure the quality of the communication and lighting of VLC systems, we optimize the proportion of power from RGB LEDs and white LEDs. We also define the optimal proportion of power. Through the above analysis, the VLC system is restricted by the following formulas

$$\mathrm{R_a} \geq 80 \tag{27}$$

$$SNR^{\mathrm{X}} \geq SNR_{\mathrm{min}} \tag{28}$$

$$BER \leq BER_{\mathrm{max}}. \tag{29}$$

IV. Numerical and Simulation Results

The simulation parameters of system are shown in Table I. The CRI of the new light source with different combinations is shown in Fig. 2. Fig. 2 (a) shows that the signal power of red LEDs can be increased without affecting the quality of light source when the power of green LEDs is enhanced. The red LEDs will improve the quality of the light source when $0 \leq \eta_{\mathrm{r}} \leq 0.026$ and then reduce the quality of light source when $\eta_{\mathrm{r}} \geq 0.026$. When only the red LEDs are used as a communication antenna with OOK modulation, η_{r} should be greater than or equal to 0.0622 and less than or equal to 0.124 according to Fig. 2 (a) and Fig. 3 (a). When η_{g}=0.2 and η_{r}=0.07, the system cannot only meet the requirements of communication using OOK modulation, but also achieve the

TABLE I
Simulation Parameters

Parameter	Value
Half intensity viewing angle, $\Phi_{1/2}$	70°
Responsivity of PD, R	0.28 A/W
Boltzmann's constant, κ_B	1.3806×10^{-23} J/K
Absolute temperature, T	295 K
Receiver FOV semiangle, Φ_c	60°
Electronic charge, q	1.602×10^{-19} C
Bandwidth, B	100 MHz
Power of white LEDs, P_{white}	20W
Area of PD, A_{APD}	1cm^2
Refractive index, c	1.5
Background current, I_{BC}	5.1 mA
Open-loop voltage gain, G_o	10
FET transconductance, g_{m}	30 mS
FET channel noise factor, Γ	1.5
Fixed capacitance of PD per unit area, μ	112 pF/cm^2
Amplifier noise density, i_{amp}	5 pA/$\sqrt{\mathrm{Hz}}$

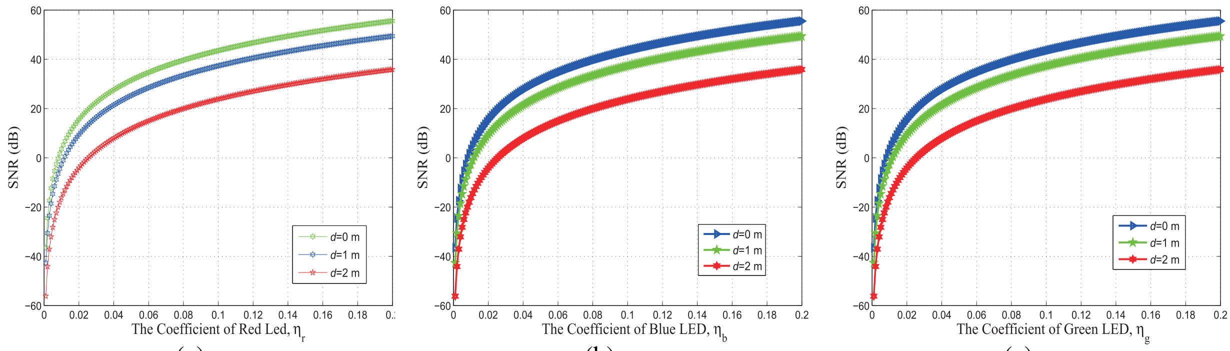

(a) (b) (c)

Fig. 3. The distribution of SNR of optical signal through different filters. (a) red filter, (b) blue filter, and (c) green filter.

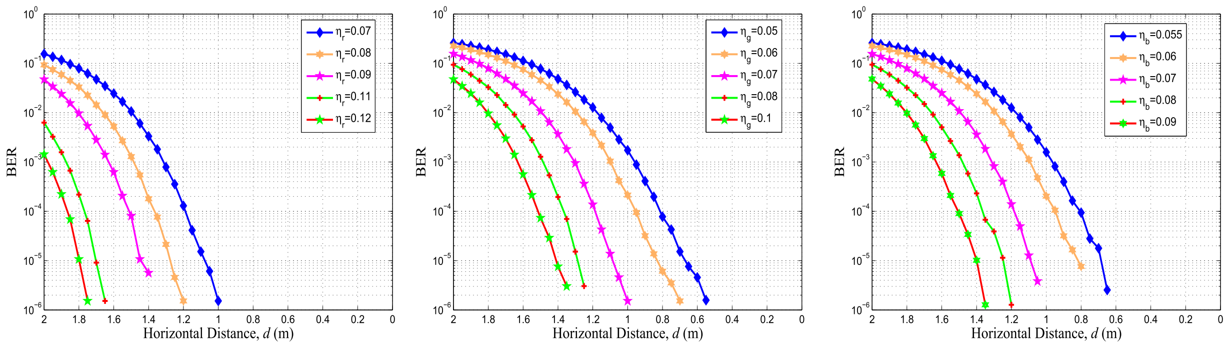

(a) (b) (c)

Fig. 4. The difference performance of BER for different sensor in the differdent positions with DCO-OFDM modulation. (a) red sensor, (b) green sensor, and (c) blue sensor.

maximum R_a.

Fig. 2 (b) shows the relationship of the combination of blue LEDs and green LEDs. The R_a decreases with the increase of the blue light power at different values of η_g. The power of blue LEDs can be enlarged when the power of green LEDs is added. However, when η_b is equal to 0.035, the R_a=89.27 does not change with the change of power of green LEDs. From Fig. 2 (b) and Fig. 3 (b), η_b should be in the range of $0.0623 \leq \eta_b \leq 0.086$ when only the blue LEDs are utilized for communication with OOK modulation. When η_g is greater than 0.8, the ability of green LEDs enhancing the quality of light source is obviously receded. R_a is increased by 5, 2, and 1, respectively, when the power ratio η_g of green LEDs increases by 0.4 each time.

Fig. 2 (c) shows that the power of blue LEDs can be enhanced for communication when the power of red LEDs is boosted. The VLC system can adaptively adjust the power of the red and blue LEDs according to the actual situation. When η_r=0.127 and η_b=0.1, R_a is equal to 99.76 and the system can obtain a good communication performance with BER$\leq 10^{-6}$ for OOK modulation.

Fig. 2 (d) shows that the influence curve of green light on R_a under the condition of $\eta_r \leq 0.12$. The R_a is always greater than 80. When η_r=0 and η_r=0.02, the power of green plays a leading role in this combination of red and green LEDs. However, when η_r=0.04, η_r=0.06, η_r=0.08, η_r=0.1, and η_r=0.12, the R_a will be first increased to 100 and then decreased slightly. The green LEDs can be used to ensure the communication signal strength of the system. For OOK modulation, η_g should be greater than 0.0623 according to Fig. 3 (c).

Fig. 4 shows the communication performance of the system using DCO-OFDM modulation in different positions of room. We used 16 quadrature amplitude modulation. In this case, the intensity of RGB LEDs is the optical signal. The average intensity is used to calculate the SNR. Under the same signal strength, the different distance d has different BER. When η_r is equal to 0.11, good communication can be achieved with BER$\leq 10^{-6}$ in the circular area of 1.6 m radius in Fig. 4 (a). When η_g is equal to 0.1, the circular area of 1.3 m radius can provide good communications with BER$\leq 10^{-6}$ in Fig. 4 (b). When η_b is equal to 0.07, the communication with BER$\leq 10^{-6}$ can be realized in the circular area of 1 m radius in Fig. 4 (c). The system can adaptively adjust the power ratio of red, green, and blue LEDs to adapt to the different requirements of communication performance and scope.

V. Conclusions

In this paper, the new light source has been theoretically demonstrated to be used for illumination and communication simultaneously. When the red or blue LEDs are solely used to communicate, the adjustable range of power is small, $\eta_r \leq 0.124$ and $\eta_b \leq 0.086$. When the green light is used for communication alone and η_b=0.8, the R_a is only reduced by 5 and $R_a \geq 80$ meeting the requirements of indoor lighting. The respective power of RGB LEDs can be adjusted to meet the requirements of optical signal strength for different scenarios and different VLC systems through different combinations. By controlling the intensity of the optical signal, the communication range can be controlled in the specified area to improve the safety and adaptability of the system. This paper provides theoretical guidance for the future selection of the light source of VLC systems.

ACKNOWLEDGMENT

The authors gratefully acknowledge the support from the Natural Science Foundation of China (No. 61371110, 61401254), Fundamental Research Funds of Shandong University (No. 2017JC029), Key R&D Program of Shandong Province (No. 2016GGX101014), Shandong Provincial Natural Science Foundation (No. ZR2017MF012), Science and Technology Project of Guangzhou (No. 201704030105), EPSRC TOUCAN project (Grant No. EP/L020009/1), and EU H2020 RISE TESTBED project (Grant No. 734325).

REFERENCES

[1] P. Pathak, X. Feng, P. Hu, and P. Mohapatra, "Visible light communication, networking and sensing: A survey, potential and challenges," *IEEE Commun. Surveys Tuts*, vol. 17, no. 4, pp. 2047–2077, 4th Quart. 2015.

[2] D. Karunatilaka, F. Zafar, V. Kalavally, and R. Parthiban, "LED based indoor visible light communications: State of the art," *IEEE Commun. Surveys Tuts*, vol. 17, no. 3, pp. 1649–1678, 3rd Quart. 2015.

[3] J. M. Luna-Rivera, R. Perez-Jimenez, J. A. Rabadan-Borjes, J. F. Rufo-Torres, V. Guerra, and C. Suarez-Rodriguez, "Multiuser scheme for indoor visible light communications using RGB LEDs," in *Proc. IWOBI'14*, Costa rica, Liberia, Jul. 2014, pp. 119–123.

[4] H. D. Chen, C. H. Wu, H. L. Li, X. B. Chen, and Z. Y. Gao, "Advances and prospects in visible light communications," *J. Semicond.*, vol. 37, no. 1, pp. 1–10, Jan. 2016.

[5] G. Cossu, A. M. Khalid, P. Choudhury, R. Corsini, and E. Ciaramella, "Long distance indoor high speed visible light communication system based on RGB LEDs," in *Proc. ACP'12*, Guangzhou, China, Nov. 2012, pp. 1–3.

[6] S. He, G. Ren, Z. Zhong, and Y. Zhao, "M-ary variable period modulation for indoor visible light communication system," *IEEE Commun. Lett.*, vol. 17, no. 7, pp. 1325–1328, Jul. 2013.

[7] S. H. Chen, and C. W. Chow, "Color-filter-free WDM MIMO RGB-LED visible light communication system using mobile-phone camera," in *Proc. ICOCN'14*, Suzhou, China, Nov. 2014, pp. 1–4.

[8] L. Cui, Y. Tang, H. Jia, J. Luo, and B. Gnade, "Analysis of the multi-channel WDM-VLC communication system," *J. Lightwave Technology*, vol. 34, no. 24, pp. 5627–5634, Dec. 2016.

[9] Y. Ohno, "Spectral design considerations for white LED color rendering," *Optical Engineering*, vol. 44, no. 11, pp. 1–9, Nov. 2013.

[10] L. Y. Chen, J. K. Chang, and W. H. Cheng. "Optical model for novel glass-based phosphor-converted white light-emitting diodes," *J. Display Technology*, vol. 9, no. 6, pp. 441–446, Jun. 2013.

[11] R. Srividya, and C. P. Kurian, "White light source towards spectrum tunable lighting - a review," in *Proc. ICAECT'14*, Manipal, India, Jan. 2014, pp. 203–208.

[12] Y. Ohno, "CIE fundamentals for color measurements," in *Proc. IS & TNIP*, Vancouver, Canada, Oct. 2000, pp. 16–20.

[13] J. Smith, "Calculating color temperature and illuminance using the TAOS TCS3414CS digital color sensor," in *INTELLIGENT OPTO SENSOR*, Feb. 2009.

[14] E. Li, W. Zhang, J. Sun, C. X. Wang, and X. Ge, "Energy-spectral efficiency tradeoff of visible light communication systems," in *Proc. ICCC'16*, Chengdu, China, Jul. 2016, pp. 1–5.

[15] M. Rahaim, and T. D. C. Little, "SINR analysis and cell zooming with constant illumination for indoor VLC networks," in *Proc. IWOW'13*, Newcastle upon Tyne, UK, Mar. 2013, pp. 20–24.

[16] T. Komine, and M. Nakagawa, "Fundamental analysis for visible-light communication system using LED lights," *IEEE Trans. Consum. Electron.*, vol. 50, no. 1, pp. 100–107, Feb. 2004.

[17] J. H. Lee, and S. Y. Jung, "SNR analyses of the multi-spectral light channels for optical wireless LED communications in intelligent transportation system," in *Proc. VTC-Spring'14*, Seoul, South Korea, May. 2014, pp. 1–5.

[18] L. Zeng, D. O'Brien, H. Le-Minh, K. Lee, D. Jung, and Y. Oh, "Improvement of date rate by using equalization in an indoor visible light communication system," in *Proc. ICCSC'08*, Shanghai, China, May. 2008, pp. 678–682.

[19] T. C. Bui, S. Kiravittaya, N. H. Nguyen, N. T. Nguyen, and K. Spirinmanwat, "LEDs configuration method for supporting handover in visible light communication," in *Proc. TENCON'14*, Bangkok, Thailand, Jan. 2014, pp. 1–6.